OPEN

Original article

Nuclear Medicine Communications

Evaluation of drug effects on cerebral blood flow and glucose uptake in un-anesthetized and un-stimulated rats: application of free-moving apparatus enabling to keep rats free during PET/SPECT tracer injection and uptake

Taku Sugita[a], Yusuke Kondo[a], Seigo Ishino[a], Ikuo Mori[a], Takashi Horiguchi[a], Mikako Ogawa[b] and Yasuhiro Magata[b]

Objectives **The purpose of this study is the development of novel fluorine-18-fluorodeoxyglucose (^{18}F-FDG)-PET and ^{99m}Tc-hexamethylpropylene amine oxime (HMPAO) SPECT methods with free-moving apparatus on conscious rats to investigate brain activity without the effects of anesthesia and tactual stimulation. We also assessed the sensitivity of the experimental system by an intervention study using fluoxetine as a reference drug.**

Materials and methods **A catheter was inserted into the femoral vein and connected to a free-moving cannula system. After fluoxetine administration, the rats were given an injection of ^{18}F-FDG or ^{99m}Tc-HMPAO via the intravenous cannula and released into a free-moving cage. After the tracer was trapped in the brain, the rats were anesthetized and scanned with PET or SPECT scanners. Then a volume of interest analysis and statistical parametric mapping were performed.**

Results **We could inject the tracer without touching the rats, while keeping them conscious until the tracers were distributed and trapped in the brain using the developed system. The effects of fluoxetine on glucose uptake and cerebral blood flow were perceptively detected by volume of interest and statistical parametric mapping analysis.**

Conclusion **We successfully developed free-moving ^{18}F-FDG-PET and ^{99m}Tc-HMPAO-SPECT imaging systems and detected detailed glucose uptake and cerebral blood flow changes in the conscious rat brain with fluoxetine administration. This system is expected to be useful to assess brain activity without the effects of anesthesia and tactual stimulation to evaluate drug effect or animal brain function.** ***Nucl Med Commun*** **39:753–760 Copyright © 2018 The Author(s). Published by Wolters Kluwer Health, Inc.**

Nuclear Medicine Communications 2018, **39:**753–760

Keywords: conscious, ^{18}F-FDG-PET, free moving, nonanesthesia, rat, ^{99m}Tc-HMPAO

[a]Pharmaceutical Research Division, Takeda Pharmaceutical Company Limited, Osaka and [b]Medical Photonics Education and Research Center, Hamamatsu University School of Medicine, Hamamatsu, Japan

Correspondence to Yasuhiro Magata, PhD, Department of Molecular Imaging, Preeminent Medical Photonics Education and Research Center (pMPERC), Hamamatsu University School of Medicine, 1-20-1 Handayama, Higashi-ku, Hamamatsu 431-3192, Japan
Tel: + 81 534 352 398; fax: + 81 534 352 393; e-mail: ymagata@hama-med.ac.jp

Received 26 February 2018 **Revised** 24 April 2018 **Accepted** 2 May 2018

Introduction

Imaging of the brain activities, including oxygen metabolism, glucose metabolism, and cerebral blood flow (CBF), has been effectively used for diagnosis, brain research, and clinical trials [1–5]. Combination of these imaging techniques and voxel-based comprehensive analysis, such as statistical parametric mapping (SPM), has been used and is useful to understand the pathophysiology of diseases and neural activity about brain function [6–8].

Imaging has been widely recognized as a translational technology because the same tracers and modalities can be used in both preclinical and clinical studies. In addition, the advantage of being noninvasive enables longitudinal evaluation of disease progress or drug effect. However, there are some discrepancies to be matched for the translational research, especially in drug evaluation using imaging biomarkers. The major discrepancy is anesthesia, which is required to immobilize the animals in preclinical studies, whereas clinical brain imaging is performed in the conscious state without anesthesia. Anesthetization before tracer injection can affect brain metabolism and CBF, and also has some interactions with central nervous system-acting drugs [9,10]. It indicates that there might be discrepancies between the imaging data and general pharmacological or pharmacokinetic data also in preclinical research. To avoid this problem, there have been some reports of preclinical imaging using pharmacological MRI, fluorine-18-fluorodeoxyglucose (^{18}F-FDG)-PET and ^{99m}Tc-hexamethylpropylene amine oxime (HMPAO)-SPECT in conscious animals [11–14].

0143-3636 Copyright © 2018 The Author(s). Published by Wolters Kluwer Health, Inc. DOI: 10.1097/MNM.0000000000000863

However, in most of these studies, the animals are exposed to the stress of physical restraint, which has a huge effect on the brain function [15–17].

In the present study, we tried to develop a new imaging system to deal with these problems, namely, we combined femoral cannulation techniques and a free-moving device commonly used for microdialysis. We implanted polyethylene cannulas into femoral veins of rats and connected them to a free-moving device, which enabled tracer injection without touching conscious rats. Regarding tracers, we used ^{18}F-FDG and ^{99m}Tc-HMPAO with a metabolic trapping mechanism so that accumulation of the tracer was kept at a steady level after uptake and distribution in the brain [18,19]. The rats were conscious during the tracer uptake period and were then anesthetized immediately before the scans, so that the image would reflect the brain condition in the conscious state based on the tracer trapping mechanism. Then, we assessed the detectability of the experimental system by the detection of the effect of fluoxetine, a selective serotonin reuptake inhibitor (SSRI). Fluoxetine was used as a reference drug because fluoxetine has been widely used in preclinical and clinical and has been reported to affect glucose metabolism in brain [20–23]. The effects of fluoxetine were investigated by volume of interest (VOI) analysis and SPM. In the ^{99m}Tc-HMPAO-SPECT study, we also calculated regional cerebral blood flow (rCBF) with VOI analysis and input function data measured by serial blood sampling.

Materials and methods

Animal preparation

Totally 52 Wistar rats (male, 13 weeks old; Japan SLC Inc., Shizuoka, Japan) were used in this study (Tables 1 and 2). Twenty-six rats were used for the ^{18}F-FDG-PET study (control, $n=12$; fluoxetine, $n=14$), and 26 rats were used for the ^{99m}Tc-HMPAO-SPECT study (control, $n=14$; fluoxetine, $n=12$). The rats were kept under environmentally controlled conditions (12-h normal light/dark cycles, 20–23°C and 50% relative humidity) with standard rat chow and water *ad libitum*. Every rat had surgical catheterization into the right femoral vein under 2–5% isoflurane anesthesia. For ^{99m}Tc-HMPAO-SPECT, the left femoral artery was also catheterized for serial blood sampling. The catheters were led out to the back of neck via subcutaneous tunnels. At least 2 days were allowed for recovery from the surgery before ^{18}F-FDG-PET and ^{99m}Tc-HMPAO-SPECT. After confirming that no abnormal behavior was noticed in the rats, they were fasted 18 h before the tracer injection (Fig. 1). The Animal Care and Use Committee of the Hamamatsu University School of Medicine approved all of the PET and SPECT studies.

Table 1 Body weight, blood glucose level and injected radioactivity in ^{18}F-FDG-PET study

	Control	Fluoxetine
Animal (*N*)	12	14
Body weight (g)	268±5	269±11
Blood glucose (mg/dl)	93±4	92±7
Injected radioactivity (μCi)	182±4	184±4

Data are mean±SEM.
There are no significant differences between the control and fluoxetine groups.
^{18}F-FDG, fluorine-18-fluorodeoxyglucose.

Tracers and drugs

Fluoxetine hydrochloride (Wako Pure Chemical Industries Ltd, Osaka, Japan, 20 mg/ml/kg suspended in 0.5% methylcellulose saline) was administered intraperitoneally 24, 19 and 1 h before injection of the tracer in both ^{18}F-FDG-PET and ^{99m}Tc-HMPAO-SPECT (Fig. 1) [14]. The control group was given 0.5% methylcellulose saline. ^{18}F-FDG was obtained from Nihon Medi-Physics Co. Ltd (Tokyo, Japan). ^{99m}Tc-HMPAO solution was synthesized immediately before the injection using a commercial kit (Cerebrotec kit; Nihon Medi-Physics Co. Ltd) and ^{99}Mo/^{99m}Tc generator (Nihon Medi-Physics Co. Ltd). The radiochemical purity was measured by thin layer chromatography (Table 2).

^{18}F-FDG-PET scan

The study protocol is depicted in Fig. 1. Initially, 75 min before ^{18}F-FDG injection, blood was sampled from the tail vein and the blood glucose was measured by a blood glucose analysis system (ACCU-CHECK compact plus; Roche Diagnostics, Basel, Switzerland). Then the rats were placed in a free-moving catheter system (Sugiyama-gen Co. Ltd, Tokyo, Japan) and habituated in the acryl cylinder cages (20 cm diameter, 30 cm height) covered with a black sheet. ^{18}F-FDG (control: 182±4 μCi, fluoxetine: 184±4 μCi, Table 1) was injected intravenously in each rat from the tip of free-moving cannula outside the cage. Thereafter, 25 min after the ^{18}F-FDG injection, the rats were anesthetized with propofol (Maruishi Pharmaceutical Co. Ltd, Osaka, Japan) and removed from the free-moving system. Then the head of each rat was fixed to an acrylic head holder (Narishige Japan Co. Ltd, Tokyo, Japan) on the animal bed of an FX preclinical platform scanner (X-O•X-PET•X-SPECT; Gamma Medica-Ideas, Northridge, Los Angeles, USA).

Table 2 Body weight, blood glucose level, blood PCO_2, blood pH, injected radioactivity, and radiochemical purity in ^{99m}Tc-HMPAO-SPECT study

	Control	Fluoxetine
Animal (*N*)	14	12
Body weight (g)	272±2	276±2
Blood glucose (mg/dl)	114±4	104±3
PCO_2 (mmHg)	38.7±0.4	40.0±1.0
pH	7.48±0.01	7.49±0.01
Injected radioactivity (mCi)	3.82±0.02	3.79±0.03
Radiochemical purity (%)	92.3±0.5	91.2±0.5

Data are mean±SEM.
There are no significant differences between the control and fluoxetine groups.
HMPAO, hexamethylpropylene amine oxime.

Fig. 1

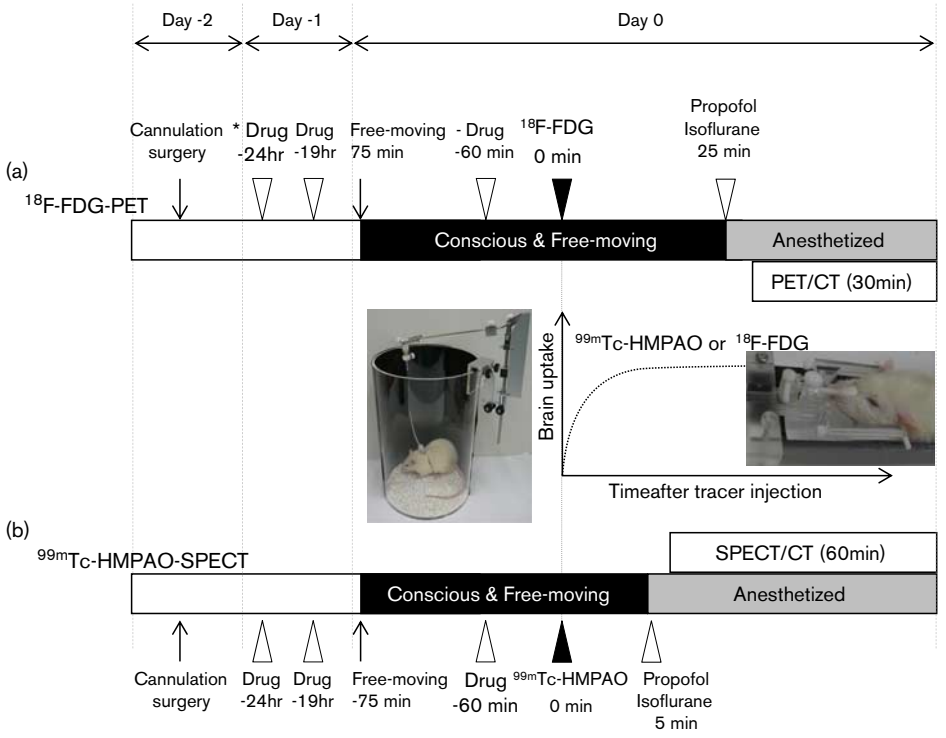

The study protocol of (a) ^{18}F-FDG-PET and (b) ^{99m}Tc-HMPAO-SPECT. The cannulation surgery was performed into the femoral vein 2 days before the scans. Control or fluoxetine was administered intraperitoneally 24, 19, and 1 h before the tracer injection. Overall, 75 min before the tracer injection, the rats were attached to the free-moving system and habituated, and then tracer was injected. (a) 25 min after ^{18}F-FDG injection, the rats were anesthetized with propofol and fixed to the animal bed of the PET scanner. Then, 30 min PET scan and sequential X-ray CT scan were performed. (b) Serial arterial blood sampling was performed for 2 min after ^{99m}Tc-HMPAO injection, and 5 min after ^{99m}Tc-HMPAO injection, the rats were anesthetized with propofol and fixed to the animal bed of SPECT scanner. Then 60-min SPECT scan and sequential X-ray CT scan were performed. CT, computed tomography; ^{18}F-FDG, fluorine-18-fluorodeoxyglucose; HMPAO, hexamethylpropylene amine oxime.

Then 30 min after the tracer injection, 30-min static PET scans were performed with 1.5% (v/v) isoflurane anesthesia and subsequent CT scans were performed with the same scanner.

Data analyses of ^{18}F-FDG-PET

^{18}F-FDG-PET tomographic images were reconstructed from the projection data using ordered-subset expectation maximization with four iterations and 15 subsets, with image matrix sizes of $256 \times 256 \times 256$ voxels and voxel sizes of $0.4 \times 0.4 \times 0.4$ mm. CT image data were reconstructed with image matrix sizes of $512 \times 512 \times 512$ voxels and voxel sizes of $0.19 \times 0.19 \times 0.19$ mm. Standardized uptake value of ^{18}F-FDG was calculated according to the following formula: brain radioactivity (kBq/ml) $\times$ body weight (g)/injected radioactivity (kBq). For VOI analysis, the radioactivity of the whole brain and each brain region was obtained using PMOD software (version 3.2, PMOD Group, Switzerland, 2009) and the accompanying VOI templates. The VOI template was modified to major 13 regions [whole brain, whole cortex, cortex (anterior), cortex (middle), cortex (posterior), midbrain, cerebellum, brain stem, hippocampus, caudate putamen, thalamus, hypothalamus, and amygdala]. The whole-brain ratio of each VOI was calculated as the ratio of the radioactivity density on each VOI to that for the whole brain. For SPM, the preprocessed PET images were coregistered and extra-brain voxels were masked. After the masking, the images were registered and analyzed using the SPM2 software package (SPM, Welcome Department of Cognitive Neurology, London, UK) with an unpaired *t*-test (threshold $P < 0.001$, height threshold at 75% of mean, extent four voxels). The anatomical regions where the PET signals changed were determined by coregistered SPM on the MRI template and the rat brain atlas [24,25].

^{99m}Tc-HMPAO-SPECT scan

The study protocol is depicted in Fig. 1. Initially, 75 min before ^{99m}Tc-HMPAO injection, blood glucose, pH and partial pressure of carbon dioxide (PCO_2) were determined with blood sampling from the tail vein by a blood glucose analysis system and blood gas analyzer (i-STAT; Abbott Laboratories, Abbott Park, Illinois, USA). Then the rats were placed in a free-moving catheter system and

habituated as described previously. ^{99m}Tc-HMPAO (control: 3.82 ± 0.02 mCi, fluoxetine: 3.79 ± 0.03 mCi, Table 2) was injected intravenously, and then serial arterial blood sampling (~25 μl) was performed at 0, 4, 8, 12, 16, 20, 24, 28, 32, 36, 40, 44, 48, 52, 56, 60, 80, 100, and 120 s after the tracer injection via a free-moving arterial cannula outside the cage. Then, 5 min after ^{99m}Tc-HMPAO injection, the rats were anesthetized with propofol and removed from the free-moving system and placed on the scanner bed. Thereafter, 10 min after the tracer injection, static SPECT scans were performed for ~60 min (1 min × 60 frames) with 1.5% (v/v) isoflurane anesthesia and subsequent CT scans were performed with the same scanner.

Data analyses in ^{99m}Tc-HMPAO-SPECT

^{99m}Tc-HMPAO-SPECT images were reconstructed from the projection data using ordered-subset expectation maximization with five iterations and four subsets, with image matrix sizes of 256 × 256 × 256 voxels and voxel sizes of 0.92 × 0.91 × 0.91 mm. CT image data were reconstructed with image matrix sizes of 60 × 60 × 60 voxels and voxel sizes of 0.17 × 0.17 × 0.17 mm. SPECT images were smoothed with a Gaussian kernel filter (full width at half maximum = 2.0 mm) and VOI analysis and SPM were performed with the same procedure as the ^{18}F-FDG-PET. rCBF was calculated from the VOI radioactivity and arterial blood radioactivity according to following formula: regional brain radioactivity (kBq/ml)/blood radioactivity $AUC_{0–26\,s}$ (kBq/ml/min) [26]. Blood outflow delay caused by the cannula length was estimated at 8 s and taken into consideration to calculate the AUC.

Statistical analyses

Data were represented as mean ± SD. Statistical analyses were performed with unpaired Student's *t*-test. *P* value of less than 0.05 was considered to be statistically significant.

Ethical approval

The study was approved by the Animal Care and Use Committee of the Hamamatsu University School of Medicine.

Results

Effect of fluoxetine on glucose uptake

There were no differences in the blood glucose levels between either groups immediately before placing in the free-moving system. The standardized uptake value of the whole brain significantly decreased in the fluoxetine group compared with the 0.5% methylcellulose saline-administered control group (5.2 ± 0.2 and 8.5 ± 0.2, respectively). The whole-brain ratio with VOI-based analysis of each brain region is shown in Table 3. Significant ^{18}F-FDG uptake increases were observed in the anterior cortex and hypothalamus (3.4%, both) in the fluoxetine group. There were significant ^{18}F-FDG uptake decreases in the posterior cortex, midbrain, brain stem and hippocampus (2.0, 6.4, 3.7 and 2.6%, respectively) after fluoxetine administration. SPM analysis showed fluoxetine-induced increased signals inside the cerebellum and decreased signals in the large brain region around the midbrain, including the periaqueductal gray (PAG), a part of the hippocampus, the parahippocampal region, and the superior and inferior colliculi (Fig. 2).

Table 3 Whole-brain ratio of fluorine-18-fluorodeoxyglucose uptake on each brain region

Brain region	Control	Fluoxetine	*P*-value	%Change
Cortex (whole)	1.13 ± 0.01	1.13 ± 0.00	0.199	0.78
Cortex (anterior)*	1.28 ± 0.01	1.32 ± 0.01	0.001	3.37
Cortex (middle)	1.20 ± 0.01	1.22 ± 0.01	0.163	1.14
Cortex (posterior)	0.97 ± 0.01	0.95 ± 0.00	0.012	−1.95
Midbrain*	1.19 ± 0.01	1.11 ± 0.00	0.000	−6.42
Cerebellum	0.86 ± 0.01	0.87 ± 0.01	0.614	0.61
Brain stem*	0.85 ± 0.01	0.82 ± 0.01	0.043	−3.67
Hippocampus*	1.24 ± 0.01	1.21 ± 0.00	0.005	−2.56
Caudate putamen	1.50 ± 0.01	1.50 ± 0.01	0.455	−0.46
Thalamus	1.26 ± 0.01	1.28 ± 0.01	0.132	1.13
Hypothalamus*	0.93 ± 0.01	0.97 ± 0.01	0.037	3.41
Amygdala	0.91 ± 0.01	0.91 ± 0.01	0.699	−0.50

Data are mean ± SEM. The regional volume of interest data were compared between the control and fluoxetine groups.
*$P < 0.05$.

Effect of fluoxetine on brain blood flow

There were no differences in the blood glucose levels, pH or PCO_2 between either groups (Table 2). Table 4 summarizes the effect of fluoxetine on rCBF calculated with VOI analysis and arterial blood radioactivity. A significant decrease of rCBF was detected in all brain regions. SPM analysis based on global mean scaling showed higher rCBF only in the bilateral small regions around the primary somatosensory cortex after fluoxetine administration (Fig. 3). In contrast, decrease in rCBF was not detected in any cluster of voxels.

Discussion

Clinical PET/SPECT imaging is generally performed without anesthesia and has the discrepancy of differences with preclinical imaging derived from the use of anesthesia. Therefore, we combined ^{18}F-FDG-PET and ^{99m}Tc-HMPAO-SPECT methodologies with a free-moving cannula system to avoid the effect of anesthesia on tracer distribution. This allowed injection of the tracers to the rats while keeping the rats conscious and free during the tracer uptake period, and then the brain metabolism or CBF could be assessed with minimum effect of anesthesia and tactual stimulation. In the present study, we evaluated the SSRI (fluoxetine) effect on brain glucose metabolism and CBF using this methodology. SPM analysis showed significant increases in ^{18}F-FDG uptake inside the cerebellum and decreases in the brain region around the midbrain including the PAG, a part of the hippocampus, the parahippocampal region,

Fig. 2

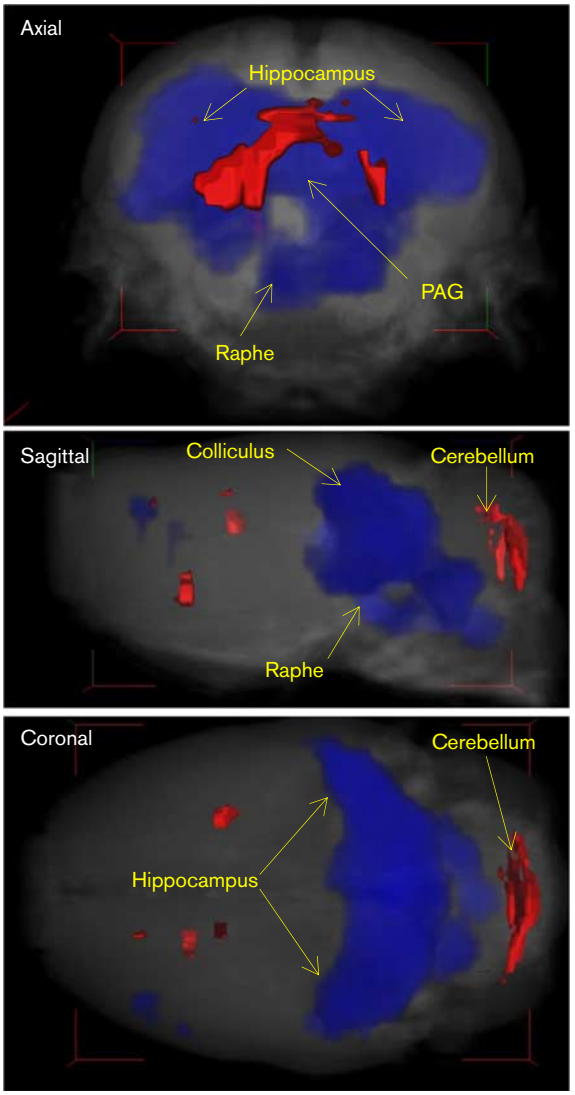

SPM images showing the effects of fluoxetine on ^{18}F-FDG uptake in the rat brain. The red region indicates the voxel clusters with significant increases and the blue region show voxel clusters with significant decreases of ^{18}F-FDG uptake compared with the control groups. ^{18}F-FDG, fluorine-18-fluorodeoxyglucose; PAG, periaqueductal gray; SPM, statistical parametric mapping.

and the superior and inferior colliculi. The regions detected have been reported to have relationship with anxiety-related diseases, such as panic disorder and obsessive-compulsive disorder [27–29]. In these reports, neuronal activity in the hippocampus, parahippocampal region and midbrain including the PAG might be decreased by SSRI or cognitive behavioral therapies; therefore, the ^{18}F-FDG uptake changes we detected could have the potential to reflect neuronal deactivation in these regions. The reason for the increased ^{18}F-FDG uptake in the cerebellum is not clear; however, apparently there might be activation compared with deactivated region in the cerebellum because motor control

Table 4 Whole-brain blood flow and regional cerebral blood flow in each brain region

Brain region	Control	Fluoxetine	*P*-value	%Change
Whole-brain blood flow*	52.8 ± 1.7	43.7 ± 1.5	0.001	−17.2
Cortex (whole)*	54.9 ± 1.7	46.5 ± 1.6	0.002	−15.2
Cortex (anterior)*	59.9 ± 1.9	51.0 ± 1.7	0.003	−14.9
Cortex (middle)*	55.8 ± 1.7	48.5 ± 1.6	0.005	−13.1
Cortex (posterior)*	50.9 ± 1.8	42.4 ± 1.5	0.002	−16.7
Midbrain*	61.0 ± 2.3	49.8 ± 1.9	0.001	−18.4
Cerebellum*	43.2 ± 1.5	36.6 ± 1.2	0.003	−15.3
Pons and medulla*	41.3 ± 3.0	28.9 ± 1.8	0.002	−30.0
Hippocampus*	63.3 ± 2.1	53.3 ± 1.9	0.002	−15.8
Caudate putamen*	75.3 ± 2.6	65.7 ± 2.3	0.012	−12.8
Thalamus*	68.6 ± 2.3	57.3 ± 2.1	0.001	−16.5
Hypothalamus*	66.5 ± 2.2	52.9 ± 2.4	0.000	−20.4
Amygdala*	60.8 ± 2.4	49.1 ± 2.1	0.002	−19.1

Data are mean ± SEM values of cerebral blood flow (ml/min 100 g). The data were compared between the control and fluoxetine groups.
*$P < 0.05$.

function in the cerebellum might be kept to control motor activity under free-moving conditions [30,31]. Interestingly, the findings in these regions are in disagreement with the serotonin transporter distribution [32,33]. These results indicate that neuronal activation or deactivation does not always occur in the site of action; therefore, function-based comprehensive analysis like the combination of ^{18}F-FDG-PET and SPM could be useful to target the region related to drug efficacy [34–37]. Furthermore, functional response itself would be an imaging biomarker especially in the case where target-specific ligand is not available [38–41].

There have been some previous reports about the effect of SSRI on rat brain. Freo *et al.* [22,23] reported detailed regional cerebral metabolic rates of glucose change by fluoxetine using ^{14}C-2-deoxy-D-glucose. In terms of the relative rate of regional cerebral metabolic rates of glucose to the whole brain, there were some regions of the brain that showed opposite changes compared with our results. Their study was performed in conscious animals, but their experimental procedure was different from our protocol, in that they immobilized the rats. In another report, Jang *et al.* [14] investigated the effect of fluoxetine on rat brain without anesthesia and physical restraint during ^{18}F-FDG uptake. They detected increased ^{18}F-FDG uptake in the dorsal hippocampus, which was different from our results. Their experimental procedure was similar to our procedure, but they restrained the rat and injected ^{18}F-FDG via the tail vein. The reasons for the differences between our results and the previous reports is not clear; however, there were methodological differences such as animal immobilization and needle stimulation, which might affect the brain activity followed by the difference of regional FDG uptake changes. These discrepancies with our result indicate the effect on brain activity and drug effect by the experimental conditions.

Fig. 3

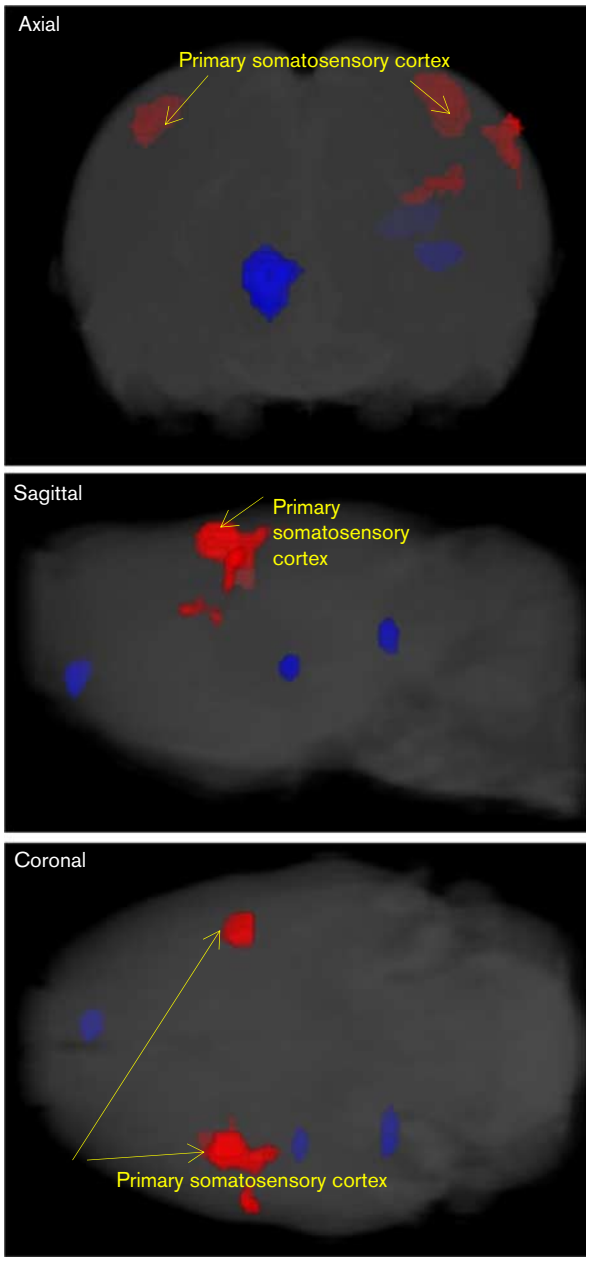

SPM images showing the effects of fluoxetine on ^{99m}Tc-HMPAO uptake in the rat brain. The red region indicates the voxel clusters with significant increases of ^{99m}Tc-HMPAO uptake compared with the control groups. HMPAO, hexamethylpropylene amine oxime; SPM, statistical parametric mapping.

SPM analysis of ^{99m}Tc-HMPAO-SPECT showed different activated regions from the ^{18}F-FDG study. We detected global CBF changes in the whole brain and relatively high rCBF only in bilateral regions around the primary somatosensory cortex, and these changes were not related to pH or PCO_2. The noncorrespondence between ^{18}F-FDG-PET and ^{99m}Tc-HMPAO-SPECT may be explained by drug-induced uncoupling [42–44]. It might reveal that region-specific ^{18}F-FDG uptake change was caused by factors other than rCBF change, such as hexokinase activity. In the ^{99m}Tc-HMPAO-SPECT study, we performed blood sampling to calculate the absolute value of CBF using blood input function. In all regions of the brain, the absolute value of rCBF decreased with fluoxetine administration. On the contrary, we used global mean scaling for SPM analysis to detect detailed comparative rCBF changes. Comparative values, such as ratio to whole brain or some reference region, are convenient to detect local changes and easy to perform, although absolute values are necessary to detect global changes. It is important to use both simple methods and rigorous methods as necessary, and our free-moving system enables use of both methods.

The effect of anesthesia and stimulation on brain activity is thought to be huge as described before. Some groups tried to minimize such effect, namely using short-time anesthesia or customized animal holders. For example, Mizuma *et al.* [12] used a customized head holder with an adapter attached to the skull and reduced the effect of stress by habituation to the experimental device. They performed ^{18}F-FDG-PET in conscious animals and obtained different images from those under anesthesia. Imaging of conscious rats immobilized with a head holder has an advantage that dynamic scanning can be performed, because the rat is restrained in the scanner during the whole experimental procedure. On the contrary, the advantage of our method is that the rats can move freely during the tracer uptake period. Actually the rats might not be completely free in aspect of catheterization and harness connection; however, we confirmed no abnormal behavior or active movement was not observed during the experiments. As there has been no gold standard imaging method under normal physiological conditions, further studies such as head-to-head comparison with other nonanesthesia method would be required to characterize our method. In spite of the future task, our free-moving methodology yet has potentials to be combined with other experimental methodologies, such as behavioral tasks, sensory stimulations, electroencephalogram or microdialysis. It would be useful to reproduce the condition of the pharmacological study to detect brain activation in specific conditions.

We used cannulation in the femoral vein and artery for tracer injection and blood sampling in the present study. Furthermore, we can easily combine additional cannulation for subcutaneous and/or intraperitoneal injection based on the same free-moving concept. In addition, this free-moving methodology has the potential to be applied for other tracers or evaluation of other drugs. Such extendibility potential is one of the appealing aspects of our methodology.

Conclusion

We successfully developed a free-moving PET and SPECT imaging system to evaluate rat brain function in conscious rats, with minimum effect of anesthesia and tactual stimulation. Using this methodology, we demonstrated that we could evaluate cerebral glucose metabolism and rCBF change by drug administration. This methodology has large extendibility such as a combination study with behavior study or other tracer application. Thus, our platform is expected to be useful to investigate drug effect and brain function.

Acknowledgements

The authors appreciate Mika Okai (Integrated Technology Research Laboratories, Takeda Pharmaceutical Company Limited) for assistance in the experimental process and data management, and Kazuhiro Hamajo (Neuroscience Drug Discovery Unit, Takeda Pharmaceutical Company Limited) and Yoshiteru Yamashita (Takeda RABICS) for animal preparation.

Conflicts of interest

There are no conflicts of interest.

References

1 Vafaee MS, Gjedde A, Imamirad N, Vang K, Chakravarty MM, Lerch JP, *et al*. Smoking normalizes cerebral blood flow and oxygen consumption after 12-hour abstention. *J Cereb Blood Flow Metab* 2015; **35**:699–705.
2 Temma T, Koshino K, Moriguchi T, Enmi J, Iida H. PET quantification of cerebral oxygen metabolism in small animals. *ScientificWorldJournal* 2014; **2014**:159103.
3 Boscolo Galazzo I, Mattoli MV, Pizzini FB, De Vita E, Barnes A, Duncan JS, *et al*. Cerebral metabolism and perfusion in MR-negative individuals with refractory focal epilepsy assessed by simultaneous acquisition of (18)F-FDG PET and arterial spin labeling. *Neuroimage Clin* 2016; **11**:648–657.
4 Welz F, Sanders JC, Kuwert T, Maler J, Kornhuber J, Ritt P1. Absolute SPECT/CT quantification of cerebral uptake of 99mTc-HMPAO for patients with neurocognitive disorders. *Nuklearmedizin* 2016; **55**:158–165.
5 Soddu A, Gómez F, Heine L, Di Perri C, Bahri MA, Voss HU, *et al*. Correlation between resting state fMRI total neuronal activity and PET metabolism in healthy controls and patients with disorders of consciousness. *Brain Behav* 2015; **6**:e00424.
6 Doruyter A, Lochner C, Jordaan GP, Stein DJ, Dupont P, Warwick JM. Resting functional connectivity in social anxiety disorder and the effect of pharmacotherapy. *Psychiatry Res* 2016; **251**:34–44.
7 Park SY, Yoon H, Lee N, Oh JK, Yoo IeR, Kim SH, *et al*. Analysis of Cerebral Blood Flow with Single Photon Emission Computed Tomography in Mild Subcortical Ischemic Vascular Dementia. *Nucl Med Mol Imaging* 2014; **48**:272–277.
8 Brendel M, Reinisch V, Kalinowski E, Levin J, Delker A, Därr S, *et al*. Alzheimer's Disease Neuroimaging Initiative. Hypometabolism in brain of cognitively normal patients with depressive symptoms is accompanied by atrophy-related partial volume effects. *Curr Alzheimer Res* 2016; **13**:475–486.
9 Chen Z, Tang J, Liu C, Li X, Huang H, Xu X, Yu H. Effects of anesthetics on vesicular monoamine transporter type 2 binding to ^{18}F-FP-(+)-DTBZ: a biodistribution study in rat brain. *Nucl Med Biol* 2016; **43**:124–129.
10 Paasonen J, Salo RA, Shatillo A, Forsberg MM, Närväinen J, Huttunen JK, *et al*. Comparison of seven different anesthesia protocols for nicotine pharmacologic magnetic resonance imaging in rat. *Eur Neuropsychopharmacol* 2016; **26**:518–531.
11 Chang PC, Procissi D, Bao Q, Centeno MV, Baria A, Apkarian AV. Novel method for functional brain imaging in awake minimally restrained rats. *J Neurophysiol* 2016; **116**:61–80.
12 Mizuma H, Shukuri M, Hayashi T, Watanabe Y, Onoe H. Establishment of in vivo brain imaging method in conscious mice. *J Nucl Med* 2010; **51**:1068–1075.
13 Hosoi R, Matsumura A, Mizokawa S, Tanaka M, Nakamura F, Kobayashi K, *et al*. MicroPET detection of enhanced ^{18}F-FDG utilization by PKA inhibitor in awake rat brain. *Brain Res* 2005; **1039**:199–202.
14 Jang DP, Lee SH, Park CW, Lee SY, Kim YB, Cho ZH. Effects of fluoxetine on the rat brain in the forced swimming test: a [F-18]FDG micro-PET imaging study. *Neurosci Lett* 2009; **451**:60–64.
15 Li C1, Li Z, Ward BD, Dwinell MR, Lombard JH, Hudetz AG, *et al*. Enhancement of resting-state fcMRI networks by prior sensory stimulation. *Brain Connect* 2014; **4**:760–768.
16 Yu X, He Y, Wang M, Merkle H, Dodd SJ, Silva AC, *et al*. Sensory and optogenetically driven single-vessel fMRI. *Nat Methods* 2016; **13**:337–340.
17 Low LA, Bauer LC, Pitcher MH, Bushnell MC. Restraint training for awake functional brain scanning of rodents can cause long-lasting changes in pain and stress responses. *Pain* 2016; **157**:1761–1772.
18 Bacciottini L, Lunghi F, Pupi A, Bonino C, Formiconi AR, De Cristofaro MT, *et al*. Evaluation of technetium 99m cyclobutylpropylene amine oxime as a potential brain perfusion imaging agent for SPET. *Eur J Nucl Med* 1990; **17**:242–247.
19 Shimoji K, Ravasi L, Schmidt K, Soto-Montenegro ML, Esaki T, Seidel J, *et al*. Measurement of cerebral glucose metabolic rates in the anesthetized rat by dynamic scanning with ^{18}F-FDG, the ATLAS small animal PET scanner, and arterial blood sampling. *J Nucl Med* 2004; **45**:665–672.
20 Kinnunen LH1, Moltz H, Metz J, Cooper M. Differential brain activation in exclusively homosexual and heterosexual men produced by the selective serotonin reuptake inhibitor, fluoxetine. *Brain Res* 2004; **1024**:251–254.
21 Bonne O1, Krausz Y, Aharon Y, Gelfin Y, Chisin R, Lerer B. Clinical doses of fluoxetine and cerebral blood flow in healthy volunteers. *Psychopharmacology (Berl)* 1999; **143**:24–28.
22 Freo U, Merico A, Ermani M, Ori C. Cerebral metabolic effects of fluoxetine, fluvoxamine, paroxetine and sertraline in the conscious rat. *Neurosci Lett* 2008; **436**:148–152.
23 Freo U1, Ori C, Dam M, Merico A, Pizzolato G. Effects of acute and chronic treatment with fluoxetine on regional glucose cerebral metabolism in rats: implications for clinical therapies. *Brain Res* 2000; **854**:35–41.
24 Schweinhardt P, Fransson P, Olson L, Spenger C, Andersson JL. A template for spatial normalisation of MR images of the rat brain. *J Neurosci Methods* 2003; **129**:105–113.
25 Paxinos G, Watson C. *The rat brain in stereotaxic coordinates*, 6th ed. Cambridge, Massachusetts: Elsevier Academic Press; 2007.
26 Suzuki C, Kimura S, Yamanaka K, Kosugi M, Magata Y. Quantitation of rat cerebral blood flow using ^{99m}Tc-HMPAO. *Nucl Med Biol*. 2017; **47**:19–22.
27 Sakai Y1, Kumano H, Nishikawa M, Sakano Y, Kaiya H, Imabayashi E, *et al*. Changes in cerebral glucose utilization in patients with panic disorder treated with cognitive-behavioral therapy. *Neuroimage* 2006; **33**:218–226.
28 Zienowicz M, Wisłowska-Stanek A, Lehner M, Taracha E, Skórzewska A, Bidziński A, *et al*. Fluoxetine attenuates the effects of pentylenetetrazol on rat freezing behavior and c-Fos expression in the dorsomedial periaqueductal gray. *Neurosci Lett* 2007; **414**:252–256.
29 Van den Heuvel OA, Veltman DJ, Groenewegen HJ, Witter MP, Merkelbach J, Cath DC, *et al*. Disorder-specific neuroanatomical correlates of attentional bias in obsessive-compulsive disorder, panic disorder, and hypochondriasis. *Arch Gen Psychiatry* 2005; **62**:922–933.
30 Stone HL, Dormer KJ, Foreman RD, Thies R, Blair RW. Neural regulation of the cardiovascular system during exercise. *Fed Proc* 1985; **44**:2271–2278.
31 Morton SM1, Bastian AJ. Mechanisms of cerebellar gait ataxia. *Cerebellum* 2007; **6**:79–86.
32 Saijo T, Maeda J, Okauchi T, Maeda J, Morio Y, Kuwahara Y, *et al*. Utility of small-animal positron emission tomographic imaging of rats for preclinical development of drugs acting on the serotonin transporter. *Int J Neuropsychopharmacol* 2009; **12**:1021–1032.
33 D'Amato RJ, Blue ME, Largent BL, Lynch DR, Ledbetter DJ, Molliver ME, *et al*. Ontogeny of the serotonergic projection to rat neocortex: transient expression of a dense innervation to primary sensory areas. *Proc Natl Acad Sci USA* 1987; **84**:4322–4326.
34 Lin WC, Chen PC, Huang YC, Tsai NW, Chen HL, Wang HC, *et al*. Dopaminergic therapy modulates cortical perfusion in parkinson disease with and without dementia according to arterial spin labeled perfusion magnetic resonance imaging. *Medicine (Baltimore)* 2016; **95**:e2206.
35 Jenkins BG. Pharmacologic magnetic resonance imaging (phMRI): imaging drug action in the brain. *Neuroimage* 2012; **62**:1072–1085.
36 Fernández-Seara MA, Aznárez-Sanado M, Mengual E, Irigoyen J, Heukamp F, Pastor MA. Effects on resting cerebral blood flow and functional connectivity induced by metoclopramide: a perfusion MRI study in healthy volunteers. *Br J Pharmacol* 2011; **163**:1639–1652.

37 Schouw ML, Kaag AM, Caan MW, Heijtel DF, Majoie CB, Nederveen AJ, *et al*. Mapping the hemodynamic response in human subjects to a dopaminergic challenge with dextroamphetamine using ASL-based pharmacological MRI. *Neuroimage* 2013; **72**:1–9.
38 Zhao F1, Williams M, Bowlby M, Houghton A, Hargreaves R, Evelhoch J, *et al*. Qualification of fMRI as a biomarker for pain in anesthetized rats by comparison with behavioral response in conscious rats. *Neuroimage* 2014; **84**:724–732.
39 Wurtman R. Biomarkers in the diagnosis and management of Alzheimer's disease. *Metabolism* 2015; **64** (**Suppl 1**):S47–S50.
40 Declercq LD, Vandenberghe R, van Laere K, Verbruggen A, Bormans G. Drug development in Alzheimer's disease: the contribution of PET and SPECT. *Front Pharmacol* 2016; **7**:88.
41 Pascoal-Faria P, Yalcin N, Fregni F. Neural markers of neuropathic pain associated with maladaptive plasticity in spinal cord injury. *Pain Pract* 2015; **15**:371–377.
42 Perthen JE, Lansing AE, Liau J, Liu TT, Buxton RB. Caffeine-induced uncoupling of cerebral blood flow and oxygen metabolism: a calibrated BOLD fMRI study. *Neuroimage* 2008; **40**:237–247.
43 Tarantini S, Hertelendy P, Tucsek Z, Valcarcel-Ares MN, Smith N, Menyhart A, *et al*. Pharmacologically-induced neurovascular uncoupling is associated with cognitive impairment in mice. *J Cereb Blood Flow Metab* 2015; **35**:1871–1881.
44 Stefanovic B, Schwindt W, Hoehn M, Silva AC. Functional uncoupling of hemodynamic from neuronal response by inhibition of neuronal nitric oxide synthase. *J Cereb Blood Flow Metab* 2007; **27**:741–754.